

11V-34
176740
P26

NASA Technical Memorandum 106166
ICOMP-93-15

Marangoni Instability in a Liquid Layer With Two Free Surfaces

Robert J. Deissler
Institute for Computational Mechanics in Propulsion
Lewis Research Center
Cleveland, Ohio

Alexander Oron
Technion-Israel Institute of Tehnology
Haifa, Israel

and

J.C. Duh
Sverdrup Technology, Inc.
Lewis Research Center Group
Brook Park, Ohio

N94-11376

Unclas

G3/34 0176740

July 1993



(NASA-TM-106166) MARANGONI
INSTABILITY IN A LIQUID LAYER WITH
TWO FREE SURFACES (NASA) 26 P





MARANGONI INSTABILITY IN A LIQUID LAYER WITH TWO FREE SURFACES

Robert J. Deissler
Institute for Computational Mechanics in Propulsion
Lewis Research Center
Cleveland, Ohio 44135

Alexander Oron
Faculty of Mechanical Engineering
Technion-Israel Institute of Technology
Haifa 32000 Israel

and

J.C. Duh
Sverdrup Technology, Inc.
Lewis Research Center Group
Brook Park, Ohio 44142

ABSTRACT

We study the onset of the Marangoni instability in a liquid layer with two free nearly insulating surfaces heated from below. Linear stability analysis yields a condition for the emergence of a longwave or a finite wavelength instability from the quiescent equilibrium state. Using the method of asymptotic expansions we derive a weakly nonlinear evolution equation describing the spatiotemporal behavior of the velocity and temperature fields at the onset of the longwave instability. The latter is given by $\Delta M = 24$, ΔM being the difference between the upper and the lower Marangoni numbers. It is shown that in some parametric range one convective cell forms across the layer, while in other parametric domains two convective cells emerge between the two free surfaces.

PACS # 47.20.-k, # 47.20.Dr, # 47.20.Ky

Corresponding Author- Dr A. Oron

Correspondent's Phone number 972-429-3474

Correspondent's FAX number 972-432-4533

I. INTRODUCTION

A quiescent liquid layer exposed to a thermal gradient can exhibit a sudden onset of fluid motion under certain conditions. When the liquid layer has one or two free surface(s) and the thermal gradient is perpendicular to the free surface(s), one of the instability sources is the surface tension dependency on temperature, also known as the Marangoni effect. Since Pearson¹ first theoretically investigated the Marangoni instability phenomenon in 1958, a great deal of attention has been given to this subject due to its important implications in various industrial processes, such as the containerless processing of crystals², the welding pool technologies³, and fluid dynamics in a low-gravity environment⁴. Various different aspects of the Marangoni instability have been studied in the literature^{1,5-14}. However, the great majority of these analyses deal with liquid layers with a bottom rigid surface and a top free surface (hereafter referred to as the rigid-free case), while little research exists on the Marangoni instability in layers with a top and a bottom free surface (hereafter referred to as the free-free case).

This physical problem of the free-free case is of significance for understanding the Marangoni instability in multilayer liquid systems^{15,16} and liquid sheets held between two gas phases¹⁷. In addition, it would enhance the fundamental understanding of the Marangoni phenomena. It should be noted that Rayleigh, in his classical work¹⁸, solved the *buoyancy*-induced thermal instability in an infinite liquid layer for three different top-bottom surfaces, i.e., the rigid-rigid, the rigid-free, and the free-free case. The influence of the top and bottom surfaces can be clearly seen in the different critical Rayleigh numbers for the onset of convection, a rigid boundary having a stabilizing effect. In addition to this effect, another factor affecting the surface tension-induced instability in the free-free case is that as the liquid layer is differentially heated, the free surface on the cold end becomes thermally destabilized while the free surface on the warm end actually provides thermal stabilization, if the case of surface tension decreasing with temperature at both surfaces is considered. It is the objective of this work to investigate the Marangoni instability in the free-free case, to establish the critical threshold for its onset, and to study the steady convection pattern slightly above the onset under certain limiting conditions.

Georis et al¹⁵ studied the Marangoni instability of a tri-layer in microgravity analytically in the linear regime and numerically in the nonlinear one under the assumption that the values of the Marangoni numbers at both free nondeformable boundaries are equal. They showed that the convection is driven by one destabilized surface while the other one is stabilizing. Funada¹⁷ investigated the Marangoni instability in a liquid sheet for both

the cases of nondeformable and deformable free surfaces, assuming that the Marangoni and Biot numbers are the same at both surfaces. The critical value of the Marangoni number was found. In particular, he showed that in the case of nondeformable free boundaries the instability is to perturbations of a finite wavelength, small wavenumber (longwave) perturbations being stable, and the critical Marangoni number depends on the Biot number. It was also found that another type of instability may emerge if the boundaries are deformable.

In this paper we study the more general problem in which the ambient phase can be different at the two surfaces. We find that under certain conditions (i.e. for small Biot number at both surfaces and for a certain range of ratio of the Marangoni numbers at the two surfaces) there is a *longwave* instability at onset. Therefore, just as in the rigid-free case for small Biot number^{8,9,11}, asymptotic methods are applied to study the weakly nonlinear effects and an evolution equation describing the spatiotemporal behavior of the convection is developed. It is found that in some parametric range, one convective cell forms across the layer like in the rigid-free case, while in other parametric domains, two convective cells emerge between the two free surfaces (which does not occur in the rigid-free case).

The plan of the paper is as follows. Section II is devoted to the problem statement. Section III deals with a linear stability analysis of the phenomenon. In Section IV we derive the evolution equation describing the spatiotemporal behavior of the film undergoing Marangoni convection. Section V presents some further results of the study and discussion.

II. PROBLEM STATEMENT

A two-dimensional incompressible liquid layer of density ρ , viscosity μ and thermal conductivity λ is considered in this paper. It is assumed that this liquid layer is bounded vertically by two free surfaces with a thickness d between them and is of infinite extent in the horizontal direction. The ambient temperature of the air above the upper free surface and below the lower free surface is kept constant at T_2 and T_1 , respectively. We assume, without loss of generality since there is no gravity, that $T_2 < T_1$. The layer of interest, therefore, is exposed to a vertical temperature gradient $-\gamma$ ($\gamma > 0$). Surface tension, σ , acting at the interfaces is assumed to be temperature-dependent

$$\begin{aligned}\sigma_\ell &= \sigma_{\ell 0} + \frac{\partial \sigma_\ell}{\partial T}(T_\ell - T_{\ell 0}) \\ \sigma_u &= \sigma_{u 0} + \frac{\partial \sigma_u}{\partial T}(T_u - T_{u 0})\end{aligned}$$

where $T_{\ell 0}$ and $T_{u 0}$ are the reference temperatures and the subscripts ℓ, u correspond respectively to the lower and upper free surfaces of the layer. We note that, as is well-known, for most liquid-gas and liquid-liquid systems surface tension decreases with temperature, i.e. $\partial\sigma/\partial T < 0$, although this is not assumed in the following analysis. The ambient environment is considered to be passive. In what follows we focus on the case of a fluid layer with nondeformable static free boundaries.

The governing equations describing the flow in the layer are:

$$\begin{aligned}\rho(u_t + uu_x + vu_y) &= -p_x + \mu(u_{xx} + u_{yy}) \\ \rho(v_t + uv_x + vv_y) &= -p_y + \mu(v_{xx} + v_{yy}) \\ u_x + v_y &= 0 \\ T_t + uT_x + vT_y &= \kappa(T_{xx} + T_{yy})\end{aligned}\tag{1a, b, c, d}$$

where (u, v, p, T) are respectively the velocity field components, pressure and temperature, and κ is the thermal diffusivity of the fluid of interest. In what follows we consider the onset of Marangoni instability from the quiescent equilibrium state. Therefore u, v can be viewed as the velocity perturbations and T can be represented as

$$T = T_\ell - \gamma(y - h_\ell) + \theta(x, y, t)$$

wherein $\theta(x, y, t)$ is a perturbation of the temperature field. Eq.(1d) then can be rewritten as

$$\theta_t + u\theta_x + v\theta_y - \gamma v = \kappa(\theta_{xx} + \theta_{yy})\tag{2}$$

The boundary conditions at the lower, $y = h_\ell$, and the upper, $y = h_u$, free surfaces (both nondeformable) are:

$$y = h_\ell : \quad v = 0\tag{3a, b, c}$$

$$\mu(u_y + v_x) + \sigma_{\ell, x} = 0$$

$$\lambda\theta_y - q_\ell\theta = 0$$

$$y = h_u :$$

$$v = 0$$

$$\mu(u_y + v_x) - \sigma_{u, x} = 0$$

$$\lambda\theta_y + q_u\theta = 0 \quad (4a, b, c)$$

Introducing $d, d^2/\kappa, \kappa/d, \rho\kappa^2/d^2, \gamma d$ as scales for length, time, velocity, pressure and temperature, respectively, one rewrites eqs.(1)-(4) in the dimensionless form:

$$u_t + uu_x + vu_y = -p_x + P(u_{xx} + u_{yy})$$

$$v_t + uv_x + vv_y = -p_y + P(v_{xx} + v_{yy})$$

$$u_x + v_y = 0$$

$$\theta_t + u\theta_x + v\theta_y - v = \theta_{xx} + \theta_{yy} \quad (5a, b, c, d)$$

$y = h_\ell :$

$$v = 0$$

$$u_y + v_x - M_\ell\theta_x = 0$$

$$\theta_y - B_\ell\theta = 0 \quad (6, a, b, c)$$

$y = h_u :$

$$v = 0$$

$$u_y + v_x + M_u\theta_x = 0$$

$$\theta_y + B_u\theta = 0 \quad (7a, b, c)$$

Here and from now on, the variables x, y, t, u, v, θ are respectively dimensionless spatial coordinates (longitudinal and transverse), time, velocity perturbations (longitudinal and transverse) and temperature deviation from the conductive equilibrium state.

The dimensionless parameters of the problem are:

$$\text{the Prandtl number } P \equiv \frac{\nu}{\kappa}$$

$$\text{the "lower" Marangoni number } M_\ell \equiv \frac{(-\frac{\partial \sigma_\ell}{\partial T})\gamma d^2}{\rho\nu\kappa}$$

$$\text{the "upper" Marangoni number } M_u \equiv \frac{(-\frac{\partial \sigma_u}{\partial T})\gamma d^2}{\rho\nu\kappa}$$

$$\text{the "lower" Biot number } B_\ell \equiv \frac{q_\ell d}{\lambda}$$

$$\text{the "upper" Biot number } B_u \equiv \frac{q_u d}{\lambda}$$

wherein q_l, q_u are the rates of heat transfer by convection at the lower and upper free surfaces, respectively.

III. LINEAR STABILITY ANALYSIS

In this section we study the stability limit of the quiescent state subject to infinitesimal perturbations, under the conditions that both free surfaces of the liquid layer are nearly insulating with regard to the temperature perturbations. An analytic expression of the critical values of the lower and upper Marangoni numbers at the onset of instability is derived. It is shown that, under certain conditions, the first unstable mode, i.e. the mode which is first amplified as the critical threshold is crossed, corresponds to a zero wavenumber, $k=0$. This behavior is similar to that of a rigid-free liquid layer with nearly insulating boundaries and indicates that the first instability is a longwave one. This fact will be used in the weakly nonlinear analysis in the next section.

Our linear analysis follows in general the analysis made by Pearson¹. Therefore, where possible, we will not go into full details. Linearizing the problem given by eqs. (5)-(7) one obtains:

$$\begin{aligned}
 u_t &= -p_x + P(u_{xx} + u_{yy}) \\
 v_t &= -p_y + P(v_{xx} + v_{yy}) \\
 u_x + v_y &= 0 \\
 \theta_t - v &= \theta_{xx} + \theta_{yy}
 \end{aligned} \tag{8a, b, c, d}$$

with the boundary conditions

$$\text{at } y = -\frac{1}{2}$$

$$\begin{aligned}
 v &= 0 \\
 u_y + v_x - M_l \theta_x &= 0 \\
 \theta_y &= 0
 \end{aligned} \tag{9a, b, c}$$

$$\text{at } y = \frac{1}{2}$$

$$\begin{aligned}
 v &= 0 \\
 u_y + v_x + M_u \theta_x &= 0
 \end{aligned}$$

$$\theta_y = 0 \quad (10a, b, c)$$

Here we have assumed the boundaries of the fluid layer to be non-deformable, located at $y = -\frac{1}{2}$ and $y = \frac{1}{2}$ and nearly insulating (i.e. $B_t, B_u \Rightarrow 0$), which corresponds to the "insulating case" considered by Pearson¹.

Eqs. (8a,b,c) can be reduced to

$$v_{xzt} + v_{yzt} = P(v_{xxxx} + 2v_{xxyy} + v_{yyyy}) \quad (11)$$

Introducing into eqs. (11),(8d),(9),(10)

$$\begin{aligned} v(x, y, t) &= F(x)\Phi(y)e^{\omega t} \\ \theta(x, y, t) &= F(x)\chi(y)e^{\omega t} \end{aligned} \quad (12)$$

one obtains

$$P(\Phi'''' - 2k^2\Phi'' + k^4\Phi) = \omega(\Phi'' - k^2\Phi) \quad (13)$$

$$\chi'' - (k^2 + \omega)\chi = -\Phi \quad (14)$$

and $F'' + k^2F = 0$, where k is the wavenumber of the perturbation in the x -direction. The boundary conditions corresponding to eqs. (9)-(10) are

at $y = -\frac{1}{2}$

$$\Phi = 0, \quad \Phi'' - k^2 M_t \chi = 0, \quad \chi' = 0 \quad (15a, b, c)$$

at $y = \frac{1}{2}$

$$\Phi = 0, \quad \Phi'' + k^2 M_u \chi = 0, \quad \chi' = 0 \quad (16a, b, c)$$

Looking for the conditions to be held at the neutral stability surface ($\omega = 0$) one obtains the following solutions for eqs.(13),(14), (15a) and (16a) :

$$\Phi = a_1 \left[\sinh(ky) - \frac{2s}{c} y \cosh(ky) \right] + a_2 \left[-\frac{s}{c} \cosh(ky) + 2y \sinh(ky) \right] \quad (17)$$

$$\begin{aligned} \chi &= a_3 \sinh(ky) + \cosh(ky) - \frac{a_1}{2} \left[\frac{y}{k} \cosh(ky) + \frac{s}{k^2 c} (y \cosh(ky) - ky^2 \sinh(ky)) \right] + \\ &\quad \frac{a_2}{2} \left[\frac{s}{kc} y \sinh(ky) + \frac{1}{k^2} (y \sinh(ky) - ky^2 \cosh(ky)) \right] \end{aligned} \quad (18)$$

where $s(k) \equiv \sinh(k/2)$ and $c(k) \equiv \cosh(k/2)$. Eqs. (15b), (15c), (16c) are now used simultaneously with eqs. (17), (18) to determine the three unknowns a_1, a_2, a_3 . These are substituted into eq. (16b) to find the neutral stability criterion:

$$M_u = \frac{b_1 M_l + b_2}{b_3 M_l + b_1} \quad (19)$$

where

$$b_1 = -8csk^4 + 32c^3s^3k^2$$

$$b_2 = 256c^3s^3k^4 \quad (20)$$

$$b_3 = (c^2 + s^2)k^3 - cs(k^4 + 3k^2) + 4c^3s^3$$

Figure 1 displays the behavior of M_u as a function of M_l and k at criticality as expressed by eqs.(19)-(20). Typically in an experiment one would change both Marangoni numbers, such as by varying the temperature gradient γ (see eq. (32)), the ratio of the lower and upper Marangoni numbers remaining nearly constant (since $\partial\sigma/\partial T$ will remain nearly constant at both the top and bottom surfaces). Therefore it is useful to plot the critical curves $M_u = M_u(k; \alpha)$, where

$$\alpha \equiv \frac{M_l}{M_u} = \frac{\partial\sigma_l/\partial T}{\partial\sigma_u/\partial T}, \quad (21)$$

which result from intersections of the surface given by eq. (19) (see fig. 1) with the planes $M_l/M_u = \alpha$ for various values of α . Substituting $M_l = \alpha M_u$ in eq. (19) and solving for M_u gives

$$M_u = \frac{-b_1(1-\alpha)}{2b_3\alpha} \left[1 \pm \sqrt{1 + \frac{4b_2b_3\alpha}{b_1^2(1-\alpha)^2}} \right] \quad (22)$$

where b_1, b_2 , and b_3 are given by eq. (20). (The functions $b_1(k), b_2(k)$ and $b_3(k)$ are found to be positive and monotonically increasing as a function of k for $k > 0$ and vanish at $k = 0$.) We note that for $\alpha = 0$, $M_u = b_2/b_1$; and that for $\alpha = 1$, $M_u = \pm\sqrt{b_2/b_3}$.

Figure 2 shows some of these curves for various α . As can be seen from these curves, at onset the instability will be either to a finite wavenumber or to zero wavenumber. So an important question is: As M_u and M_l are changed while keeping α constant, such as by increasing the temperature gradient γ , under what conditions will the first instability be to a finite wavenumber and under what conditions will it be to zero wavenumber? To

find this condition, it is useful to look at the longwave limit ($k \Rightarrow 0$) of eq. (22) which is found to be (for - sign in eq. (22) and $\alpha \neq 1$)

$$M_u = \frac{24}{1-\alpha} + \frac{8(3-7\alpha+3\alpha^2)}{5(1-\alpha)^3} k^2 \quad (23)$$

The other root corresponding to the plus sign diverges as $360(1-1/\alpha)k^{-2}$ for $k \Rightarrow 0$. Since we are mainly interested in the zero wavenumber instability, we will focus our attention on the root given by eq. (23). There are two primary cases to consider: $\alpha < 1$ which at the onset of the longwave instability corresponds to $M_u > 0$; and $\alpha > 1$ which corresponds there to $M_u < 0$.

Case $\alpha < 1$: If the coefficient of k^2 is negative in eq. (23), the critical curve $M_u(k; \alpha)$ will initially decrease as k is increased from zero. It will then eventually increase as k is increased further, as given by eq. (22) and seen in fig. 2a. Therefore, as M_u is gradually increased toward the critical curve from below, the first instability will be to finite wavenumber, since the minimum of the curve is at finite k . However, if the coefficient of k^2 is nonnegative, the critical curve $M_u(k; \alpha)$ will increase as k is increased from zero. It then continues to increase monotonically as k is further increased as seen in figs. 2a,c. Therefore, as M_u is gradually increased toward the critical curve from below, the first instability will be to zero wavenumber, since the minimum of the curve is at $k = 0$.

Case $\alpha > 1$: If the coefficient of k^2 is positive in eq. (23), the critical curve $M_u(k; \alpha)$ will initially increase as k is increased from zero. It will then eventually decrease as k is increased further, as given by eq. (22) and seen in fig. 2b. Therefore, as M_u is gradually decreased toward the critical curve from above, the first instability will be to finite wavenumber, since the maximum of the curve is at finite k . However, if the coefficient of k^2 is nonpositive, the critical curve $M_u(k; \alpha)$ will decrease as k is increased from zero. It then continues to decrease monotonically as k is further increased as seen in fig. 2b. Therefore, as M_u is gradually decreased toward the critical curve from above, the first instability will be to zero wavenumber, since the maximum of the curve is at $k = 0$.

Examining the coefficient of k^2 in eq. (23) we thus find that the first instability will be to *zero* wavenumber if

$$\alpha \leq \frac{7-\sqrt{13}}{6} \cong 0.56574 \quad \text{or} \quad \alpha \geq \frac{7+\sqrt{13}}{6} \cong 1.76759 \quad (24)$$

in which case the onset of instability will occur at

$$M_u - M_l = 24 \quad (25)$$

where α is defined in eq. (21). Eq. (25) was found from taking $k = 0$ in eq. (23) and replacing α by M_ℓ/M_u . From eq. (23) for $k = 0$ and eq. (24) we see that the limits on M_u at a zero wavenumber instability are

$$-31.2666 \cong 12(1 - \sqrt{13}) \leq M_u \leq 12(1 + \sqrt{13}) \cong 55.2666 \quad (26)$$

In contrast, the first instability will be to *finite* wavenumber when

$$\frac{7 - \sqrt{13}}{6} < \alpha < \frac{7 + \sqrt{13}}{6} \quad (27)$$

We note that when $\partial\sigma/\partial T$ is the same for the upper and lower surfaces, which corresponds to $\alpha = 1$, M_u diverges as $24\sqrt{15}k^{-1}$ as $k \Rightarrow 0$ and has a minimum at finite k , corresponding to a finite wavenumber instability,¹⁷ which is included in condition (27). We also note that the root corresponding to the plus sign in eq. (22), which as noted above diverges as $k \Rightarrow 0$, corresponds to a finite wavenumber instability.

In the limit $k \Rightarrow \infty$ all neutral curves from eq. (22) are found to be given by

$$M_u \sim 8k^2 \quad \text{or} \quad M_u \sim -\frac{8}{\alpha}k^2 \quad (28)$$

the former giving the limiting behavior of the curves for which $M_u > 0$ and the latter giving the limiting behavior of the curves for which $M_u < 0$. The former is similar to the behavior found by Pearson for rigid-free boundary conditions.¹

Figures 3a and 3b give the critical values of the Marangoni number and wavenumber, $M_{u,c}$ and k_c , respectively, at which instability first sets in as a function of α . These values correspond to the minimum or maximum (depending on whether $M_u > 0$ or $M_u < 0$) of the curves given in Fig. 2. For the case $\alpha < 0$, as seen in Fig. 2c, only the lower of the two curves for a given value of α is relevant, instability occurring when M_u is above the minimum of the curve. M_u being above the minimum of the upper of the two curves for a given $\alpha < 0$ simply corresponds to there being a band of stable wavenumbers, the system as a whole still being unstable. The critical value of the upper Marangoni number, $M_{u,c}$, exists for all values of α , when $M_u > 0$. In contrast, $M_{u,c}$ exists only for positive α increasing indefinitely for $\alpha \Rightarrow 0$ when $M_u < 0$. Let us reiterate that as follows from our previous analysis and also from inspection of Fig. 3b, the first instability given by the $M_u > 0$ branch is to zero wavenumber for $\alpha < 0.56574$ and to finite wavenumber otherwise. For the $M_u < 0$ branch the first instability is to zero wavenumber for $\alpha > 1.76759$ and to finite wavenumber otherwise.

A particular case of interest is the one when surface tension at the lower free surface is temperature independent: $M_\ell = 0$ ($\alpha = 0$). Then the critical condition for the longwave instability is $M_u = 24$. The corresponding critical Marangoni number for the case of the upper free surface and the lower rigid plane was found by Pearson¹: $M = 48$. In our case (free-free) the critical Marangoni number is lower than in the Pearson's (rigid-free) case. The reason is that a rigid boundary provides a certain damping for the emerging instability although generated at the opposite boundary.

IV. WEAKLY NONLINEAR ANALYSIS.

We turn now to the weakly nonlinear analysis of stability of a quiescent state of a fluid layer of uniform thickness (we neglect the deformability of the free surfaces in what follows) which is heated from below and is subject to surface tractions due to surface tension gradients. As stated before, we will focus on the case of nearly insulating free surfaces. The equilibrium temperature distribution corresponding to the quiescent conductive state in the fluid layer is

$$T = T_1 - B_u(T_1 - T_2) \frac{B_\ell y + 1}{B_\ell + B_u(1 + B_\ell)} \quad (31)$$

Here we assumed the liquid layer to be contained between $y = 0$ and $y = 1$, for convenience.

The equilibrium temperature gradient across the layer, $\gamma = (T_\ell - T_u)/d$, is therefore

$$\gamma = \frac{B_u B_\ell (T_1 - T_2)}{d[B_\ell + B_u(1 + B_\ell)]} \quad (32)$$

Introduce the stretched spatial and temporal variables by

$$\zeta = x\sqrt{\epsilon} \quad , \quad \eta = y \quad , \quad \tau = \epsilon^2 t \quad (33)$$

where ϵ is a small perturbation parameter measuring the distance above onset [see eq. (36c,d)]. Note that the variable x is stretched, whereas the variable y is not stretched, which is consistent with a longwave instability slightly above onset [also see discussion following eq. (58)]. The Biot numbers of the system are assumed to be small and of order ϵ^2 as

$$B_u = \epsilon^2 \beta_u \quad , \quad B_\ell = \epsilon^2 \beta_\ell \quad (34)$$

The appropriate scalings for the streamfunction of the perturbation flow, Ψ , and for the deviation of the temperature from the equilibrium, eq.(31) are¹¹

$$\psi = \sqrt{\epsilon}\Psi \quad (35)$$

$$\Theta = \theta$$

The scaled variables, then, Ψ and θ are expanded in powers of ϵ :

$$\Psi = \Psi_0 + \epsilon\Psi_1 + \epsilon^2\Psi_2 + \dots$$

$$\Theta = \Theta_0 + \epsilon\Theta_1 + \epsilon^2\Theta_2 + \dots$$

$$M_\ell = M_{\ell 0} + \epsilon M_{\ell 1} + \dots$$

$$M_u = M_{u 0} + \epsilon M_{u 1} + \dots \quad (36a, b, c, d)$$

wherein $M_{\ell 0}, M_{u 0}$ represent respectively the values of the lower and the upper Marangoni number at criticality. There is still an arbitrariness in the definition of ϵ which can be removed by assuming a value for $M_{u 1}$ or $M_{\ell 1}$ (or some linear combination of them). For example, taking $M_{u 1} = M_{u 0}$ gives $\epsilon = (M_u - M_{u 0})/M_{u 0}$.

Eliminating the pressure terms from eqs.(5)-(7) and introducing the scaling (35) yields:

$$\epsilon^3\Psi_{\zeta\zeta\tau} + \epsilon^2\Psi_{\eta\eta\tau} + [\epsilon\Psi_\eta\Psi_{\zeta\eta\eta} - \epsilon\Psi_\zeta\Psi_{\eta\eta\eta} + \epsilon^2\Psi_\eta\Psi_{\zeta\zeta\zeta} - \epsilon^2\Psi_\zeta\Psi_{\zeta\zeta\eta}] =$$

$$P(\epsilon^2\Psi_{\zeta\zeta\zeta\zeta} + 2\epsilon\Psi_{\zeta\zeta\eta\eta} + \Psi_{\eta\eta\eta\eta})$$

$$\epsilon^2\Theta_\tau + \epsilon\Psi_\eta\Theta_\zeta - \epsilon\Psi_\zeta\Theta_\eta + \epsilon\Psi_\zeta = \epsilon\Theta_{\zeta\zeta} + \Theta_{\eta\eta} \quad (37a, b)$$

$\eta = 0$:

$$\Psi = 0$$

$$-(\Psi_{\eta\eta} - \epsilon\Psi_{\zeta\zeta}) + M_\ell\Theta_\zeta = 0$$

$$\Theta_\eta - \epsilon^2\beta_l\Theta = 0 \quad (38a, b, c)$$

$\eta = 1$:

$$\Psi = 0$$

$$(\Psi_{\eta\eta} - \epsilon\Psi_{\zeta\zeta}) + M_u\Theta_\zeta = 0$$

$$\Theta_\eta + \epsilon^2\beta_u\Theta = 0 \quad (39a, b, c)$$

Introducing the expansions (36) into eqs. (37)-(39) yields in the leading order

$$\begin{aligned}\Psi_{0\eta\eta\eta\eta} &= 0 \\ \Theta_{0\eta\eta} &= 0\end{aligned}\tag{40a, b}$$

$\eta = 0$:

$$\begin{aligned}\Psi_0 &= 0 \\ \Psi_{0\eta\eta} - M_{l0}\Theta_{0\zeta} &= 0 \\ \Theta_{0\eta} &= 0\end{aligned}\tag{41a, b, c}$$

$\eta = 1$:

$$\begin{aligned}\Psi_0 &= 0 \\ \Psi_{0\eta\eta} + M_{u0}\Theta_{0\zeta} &= 0 \\ \Theta_{0\eta} &= 0\end{aligned}\tag{42a, b, c}$$

A solution of eqs. (40b), (41c), (42c) is given by

$$\Theta_0 = f(\zeta, \tau)\tag{43}$$

where this function is as yet unknown. Further, an evolution equation in terms of $f(\zeta, \tau)$, describing the spatiotemporal behavior of the flow and the temperature fields, will be derived. A solution for the leading order of the streamfunction, Ψ_0 , is given by

$$\Psi_0 = (A_3\eta^3 + A_2\eta^2 + A_1\eta)f'\tag{44}$$

where

$$A_1 = -\frac{1}{3}M_{l0} + \frac{1}{6}M_{u0} \quad , \quad A_2 = \frac{1}{2}M_{l0} \quad , \quad A_3 = -\frac{1}{6}(M_{l0} + M_{u0})$$

and prime denotes differentiation with respect to ζ .

The velocity field, therefore, at this order of approximation is

$$\begin{aligned}u_0 &= \Psi_{0\eta} = (3A_3\eta^2 + 2A_2\eta + A_1)f' \\ v_0 &= -\Psi_{0\zeta} = (A_3\eta^3 + A_2\eta^2 + A_1\eta)f''\end{aligned}\tag{45a, b}$$

Along the free boundaries the velocities are

$$\eta = 0 \quad : \quad u_0 = A_1f' \quad , \quad v_0 = 0\tag{46}$$

$$\eta = 1 : \quad u_0 = (3A_3 + 2A_2 + A_1)f' , \quad v_0 = 0 \quad (47)$$

Integrating eq.(37b) at the leading order between the free surfaces with respect to η and using eqs. (43), (44) one obtains the condition to be held at criticality:

$$M_{u0} - M_{\ell 0} = 24 \quad (48)$$

which coincides with the relation found using linear stability analysis in the previous section, eq.(25).

At the first order of approximation one obtains

$$\begin{aligned} \Psi_{1\eta\eta\eta\eta} &= -2\Psi_{0\zeta\zeta\eta\eta} + \frac{1}{P}(\Psi_{0\eta}\Psi_{0\zeta\eta\eta} - \Psi_{0\zeta}\Psi_{0\eta\eta\eta}) \\ \Theta_{1\eta\eta} &= -\Theta_{0\zeta\zeta} + \Psi_{0\eta}\Theta_{0\zeta} + \Psi_{0\zeta} \end{aligned} \quad (49a, b)$$

with the boundary conditions

$\eta = 0 :$

$$\begin{aligned} \Psi_1 &= 0 \\ -\Psi_{1\eta\eta} + M_{\ell 1}\Theta_{0\zeta} + M_{\ell 0}\Theta_{1\zeta} + \Psi_{0\zeta\zeta} &= 0 \\ \Theta_{1\eta} &= 0 \end{aligned} \quad (50a, b, c)$$

$\eta = 1 :$

$$\begin{aligned} \Psi_1 &= 0 \\ \Psi_{1\eta\eta} + M_{u1}\Theta_{0\zeta} + M_{u0}\Theta_{1\zeta} - \Psi_{0\zeta\zeta} &= 0 \\ \Theta_{1\eta} &= 0 \end{aligned} \quad (51a, b, c)$$

The solution for the temperature Θ_1 is given by

$$\Theta_1 = \frac{1}{12}f'^2(6A_1\eta^2 + 4A_2\eta^3 + 3A_3\eta^4) + \frac{1}{60}f''(-30\eta^2 + 10A_1\eta^3 + 5A_2\eta^4 + 3A_3\eta^5) + q(\zeta, \tau) \quad (52)$$

where $q(\zeta, \tau)$ is an arbitrary function. The streamfunction Ψ_1 is determined via

$$\begin{aligned} \Psi_1 &= \frac{A_3^2}{70P}f'f''\eta^7 + \frac{A_2A_3}{30P}f'f''\eta^6 + \left(\frac{A_2^2}{30P}f'f'' - \frac{A_3}{10}f'''\right)\eta^5 + \\ &\left(\frac{A_1A_2}{12P}f'f'' - \frac{A_2}{6}f'''\right)\eta^4 + g_3\eta^3 + (M_{l1}f' + M_{l0}q')\frac{\eta^2}{2} + g_1\eta \end{aligned} \quad (53)$$

where

$$\begin{aligned}
g_1 = & (M_{u1} - 2M_{t1})\frac{f'}{6} + (M_{u0} - 2M_{t0})\frac{q'}{6} + \\
& \left(\frac{M_{u0}}{3} + \frac{A_1 A_2}{12P} + \frac{7A_2^2}{90P} + \frac{2A_2 A_3}{15P} + \frac{3A_3^2}{35P}\right)f' f'' + \\
& \left[-\frac{A_1}{6} - \frac{A_2}{3} - \frac{2A_3}{5} + M_{u0}\left(-\frac{1}{12} + \frac{A_1}{36} + \frac{A_2}{72} + \frac{A_3}{120}\right)\right]f''' \quad (54)
\end{aligned}$$

and

$$\begin{aligned}
g_3 = & -\frac{M_{t1} + M_{u1}}{6}f' - \frac{M_{t0} + M_{u0}}{6}q' - \left(\frac{M_{u0}}{3} + \frac{A_1 A_2}{6P} + \frac{A_2^2}{9P} + \frac{A_2 A_3}{6P} + \frac{A_3^2}{10P}\right)f' f'' \\
& + \left[\frac{A_1}{6} + \frac{A_2}{2} + \frac{A_3}{2} + \frac{M_{u0}}{12}\left(1 - \frac{A_1}{3} - \frac{A_2}{6} - \frac{A_3}{10}\right)\right]f''' \quad (55)
\end{aligned}$$

To simplify eqs. (54), (55); eq. (48) and the ensuing identity $A_1/2 + A_2/3 + A_3/4 = 1$ was used.

The evolution equation for the temperature disturbance $f(\zeta, \tau)$ is derived by integrating eq.(37b) at the order ϵ^2 with respect to η across the layer:

$$f_\tau + \int_0^1 d\eta (f' \Psi_{1\eta} + \Psi_{0\eta} \Theta_{1\zeta} - \Psi_{0\zeta} \Theta_{1\eta} + \Psi_{1\zeta} - \Theta_{1\zeta\zeta}) + (\beta_u + \beta_\ell)f = 0 \quad (56)$$

Introducing eqs.(44), (52), (53) into eq.(56) yields the key result of the work

$$f_\tau + \pi_1 f'''' + \pi_2 f'' + \beta f - \pi_3 (f'^3)' + \pi_4 (f'^2)'' = 0 \quad (57)$$

where the coefficients are given by

$$\begin{aligned}
\beta &= \beta_\ell + \beta_u \\
\pi_1 &= \frac{1}{5} + \frac{M_{u0}}{360} - \frac{M_{u0}^2}{8640} \\
\pi_2 &= \frac{M_{u1} - M_{t1}}{24} \\
\pi_3 &= \frac{1}{105} \left(128 - \frac{M_{u0}}{3} + \frac{M_{u0}^2}{72}\right) \\
\pi_4 &= \frac{11}{10} \left(\frac{1}{2} + \frac{1}{7P}\right) \left(\frac{M_{u0}}{12} - 1\right) \quad (58)
\end{aligned}$$

It is readily shown that the coefficient π_1 is positive in the range $12(1 - \sqrt{13}) < M_{u0} < 12(1 + \sqrt{13})$ which constitutes the range of validity of the present nonlinear theory and

which coincides with eq.(26) for the range of M_u for which onset is to zero wavenumber. Moreover, π_3 is always positive. On the other hand, the π_2 -term provides instability to the considered system, if $\pi_2 > 0$, i.e. $M_{u1} - M_{\ell1} > 0$. In this case, the difference between the upper and the lower Marangoni numbers, ΔM , is

$$\Delta M = M_u - M_\ell = M_{u0} - M_{\ell0} + \epsilon(M_{u1} - M_{\ell1}) > 24$$

and the layer of interest is unstable with respect to longwave perturbations, in the specified range of M_{u0} as also follows from the linear stability analysis brought in the previous section.

Also, as follows from eqs. (57), (58) and independently from the linear analysis, the linear stage of the evolution of an infinitesimal temperature disturbance is not affected by the value of the Prandtl number, P , which appears only in the nonlinear π_4 - term.

Eq. (57) and its various particular cases have recently appeared in the literature ^{8,11,14,19-22}. Ref.14 is particularly devoted to a study of eq. (57). By rescaling the spatial, temporal and dependent variables, ζ, τ, f respectively,

$$\zeta \Rightarrow \zeta \pi_1^{1/2} \pi_2^{-1/2}, \quad \tau \Rightarrow \tau \pi_1 \pi_2^{-2}, \quad f \Rightarrow f \pi_1^{1/2} \pi_3^{-1/2}$$

one obtains the equation

$$f_\tau + f'''' + f'' + sf - (f'^3)' + \omega(f'^2)'' = 0 \quad (59)$$

in the domain $0 \leq \zeta \leq L$ wherein

$$s = \beta \pi_1 \pi_2^{-2}, \quad \omega = 2\pi_4 \pi_1^{-1/2} \pi_3^{-1/2}$$

We note that eq. (59) can be recast into the form

$$f_\tau + [(1 - f'^2)f']' + f'''' + sf + \omega(f'^2)'' = 0 \quad (60)$$

The cubic term f'^3 in eq. (59) is shown to ensure the emergence of bounded amplitude patterns. Moreover, in the case of $\omega = 0$ corresponding to $M_{u0} = 12$, eq. (59) is symmetric under the transformation $f \Rightarrow -f$ and has a Lyapunov functional bounded from below (if $s > 0$) such that eq. (59) can be rewritten in the form:

$$f_\tau = -\frac{\delta F}{\delta f} \quad (61)$$

with a free energy functional given by

$$F = \int_{\Delta} \left[\frac{s}{2} f^2 + \frac{1}{4} f'^4 - \frac{1}{2} f'^2 + \frac{1}{2} f''^2 \right] dx \quad (62)$$

and Δ being either the periodic or infinite domain.

V. FURTHER RESULTS AND DISCUSSION

Turning back to the leading order of the streamfunction Ψ_0 , eq.(44), one finds that the polynomial $A_3\eta^3 + A_2\eta^2 + A_1\eta$ has three roots:

$$\eta_1 = 0, \eta_2 = 1, \eta_3 = \frac{2M_{\ell 0} - M_{u0}}{M_{u0} + M_{\ell 0}} = \frac{M_{u0} - 48}{2M_{u0} - 24} \quad (63)$$

For $M_{u0} > 48$ or $M_{u0} < -24$, η_3 lies in the domain $0 < \eta < 1$, and therefore, two different cells across the layer are expected to form, one below the other. This can be also understood from the fact, that for $M_{u0} > 48$ both the velocities at the free surfaces, $u_0(\eta = 1)$ and $u_0(\eta = 0)$, given by eqs. (46), (47) are negative when $f' > 0$, and positive otherwise. For $M_{u0} < -24$ both $u_0(\eta = 0)$ and $u_0(\eta = 1)$ are positive for positive $f' > 0$, and negative otherwise.

In contrast, for $-24 < M_{u0} < 48$ the velocities at the free boundaries have different signs, leading to formation of a single convective cell across the layer between the adjacent extrema of $f(\zeta, \tau)$. The effect of the emergence of two convective cells across the layer is novel and is not observed in the "rigid-free" case⁸.

It also readily follows from eq.(63) that for $M_{u0} > 48$ the lower cell is smaller than the upper one. If $M_{u0} < -24$ the upper cell is smaller than the lower one. These considerations are observed in our numerical study of eq.(57) as well.

Equation (57) is solved numerically using a time-splitting method together with the periodic boundary conditions in the domain $0 \leq \zeta \leq L = 5\pi$. The value of the Prandtl number is chosen as $P = 5$ which corresponds to water. The distance from the criticality expressed by the difference $M_{u1} - M_{\ell 1}$ is taken as 6. Equation (57) is amended with the initial condition related to the fundamental mode $f_0(\zeta) = 0.01 \sin(2\pi\zeta/L)$.

Figure 4a presents the solution for eq.(57), f , the leading order of the temperature disturbance, for $M_{u0} = 54, M_{\ell 0} = 30, \beta = 0$. The corresponding flow field is displayed in Fig.4b. [The streamlines shown in Figs. 4b, 5b, and 6b were calculated using eq. (44).] As explained above, two convective cells emerge across the layer, the lower cell being smaller

than the upper one. The latter can be understood from the fact that the strength of surface tractions at the upper surface is higher than that at the lower one, $|M_{u0}| > |M_{\ell 0}|$. The direction of the flow at both surfaces (see eqs. (46,47)) is from the hottest spot at the surfaces corresponding to the maximum of f (see fig. 4a) to the coldest one corresponding to the minimum of f , in agreement with the direction of the surface shear stress arising from the local variation of surface tension. Note that the temperature of the fluid is given to the leading order by $T(y) + f(\zeta, \tau)$, where the first term is the linear equilibrium state, (eq. (31)) and the second one is obtained from solving eq. (57). At this order of approximation, therefore, the temperature varies coherently along the free boundaries and the hottest and the coldest spots on each of them are located at the same vertical cross-section.

Figure 5a shows the solution for eq. (57) with $M_{u0} = -30, M_{\ell 0} = -54, \beta = 0$. The corresponding flow field is displayed in Fig. 5b. In this case, $|M_{\ell 0}| > |M_{u0}|$, and the lower cell is larger than the upper one. The direction of the flow at both surfaces is from the coldest spot at the surfaces corresponding to the minimum of f toward the hottest one corresponding to the maximum of f (see fig. 5a).

A third type of flow is presented in Figs. 6a and 6b. The parameter values taken here are $M_{\ell 0} = -12, M_{u0} = 12, \beta = 0$. This set of parameters corresponds to $\pi_4 = 0$, therefore the solution obtained is symmetric with respect to the midplane. The steady pattern for the temperature disturbance is displayed in the first and the flow field which consists of one convective cell across the layer is displayed in the second. The direction of the flow along the lower free surface is from the coldest spot to the hottest one (due to the negative Marangoni number) and the flow along the upper free surface is from the hottest spot to the coldest one.

In this paper we have studied the onset of the Marangoni instability in a liquid layer vertically bounded by two free nearly insulating surfaces with arbitrary interfacial properties. Using the linear stability analysis, we found the stability (instability) domains in the parametric space including the disturbance wavenumber and the both Marangoni numbers. In particular we derived the criterion for the first instability being to zero or to finite wavenumber. The critical threshold for the onset of the longwave instability is found to be given by the relationship between the upper and lower Marangoni numbers : $M_u - M_\ell = 24$. A weakly nonlinear analysis is applied to study the spatiotemporal evolution of the flow and temperature fields at the onset of the longwave instability. It was shown that in some parametric range one convective cell forms across the layer while in other parametric domains two convective cells emerge between the two free surfaces.

ACKNOWLEDGEMENTS

A.O. acknowledges the hospitality and the support of the Space Experiments Division and the Institute for Computational Mechanics in Propulsion (ICOMP) at NASA Lewis Research Center in Cleveland where most of the present work was done. His work is partially supported by the V.P.R. Technion Israel-Mexico Energy Research Fund and the Fund for the Promotion of Research at the Technion. The authors wish to thank Dr. R. Balasubramaniam for many stimulating discussions.

REFERENCES

- ¹ J. R. A. Pearson, *On convection cells induced by surface tension*, J. Fluid Mech., 4, 489 (1958).
- ² D. Schwabe, *Surface tension-driven flow in crystal growth melts*, Crystals-11, Springer-Verlag, 76 (1988).
- ³ G. M. Oreper and J. Szekely, *Heat and fluid flow phenomena in weld pools*, J. Fluid Mech. 147, 53 (1984).
- ⁴ S. Ostrach, *Low-gravity fluid flows*, Ann. Rev. Fluid Mech., 14, 313 (1982).
- ⁵ L. E. Scriven and C. V. Sternling, *On cellular convection driven by surface tension gradients: effects of mean surface tension and surface viscosity*, J. Fluid Mech., 19, 321 (1964).
- ⁶ D. A. Nield, *Surface tension and buoyancy effects in cellular convection*, J. Fluid Mech., 19, 341 (1964).
- ⁷ V. G. Levich and V. S. Krylov, *Surface tension-driven phenomena*, Ann. Rev. Fluid Mech., 1, 293 (1969).
- ⁸ G.I. Sivashinsky, *Large cells in nonlinear Marangoni convection*, Physica 4D, 227 (1982).
- ⁹ P. L. Garcia -Ybarra, J. L. Castillo and M. G. Velarde, *Benard- Marangoni convection with a deformable interface and poorly conducting boundaries*, Phys. Fluids, 30, 2655 (1987).
- ¹⁰ S. H. Davis, *Thermocapillary instabilities*, Ann. Rev. Fluid Mech., 19, 403 (1987).
- ¹¹ A. Oron and P. Rosenau, *Evolution of the coupled Benard- Marangoni convection*, Phys. Rev. A 39, 2063 (1989).
- ¹² A. Oron and P. Rosenau, *Formation of patterns induced by thermocapillarity and gravity*, J. Phys. (France) II , 2, 131 (1992).
- ¹³ R. J. Deissler and A. Oron, *Stable localized patterns in thin liquid films*, Phys. Rev. Letts. 68, 2948 (1992).
- ¹⁴ A. Oron, P. Rosenau and S. Gutman, in preparation.
- ¹⁵ P. Georis, M. Hennenberg, J. C. Legros, A. A. Nepomnyashchy, I. B. Simanovskii and I. I. Wertgeim, *Thermocapillary instability in a multilayer system*, 1st Int. Symp. Hydrodyn. and Heat and Mass Trans. in Microgravity, p. 105 (1991).
- ¹⁶ S. Wahal and A. Bose, *Rayleigh- Benard and interfacial instabilities in two immiscible liquid layers*, Phys. Fluids, 31, 3502 (1988).

- ¹⁷ T. Funada, *Marangoni instability in thin liquid sheet*, J. Phys. Soc. Japan, **55**, 2191 (1986).
- ¹⁸ Lord Rayleigh, *On convective currents in a horizontal layer of fluids, when the higher temperature is on the under side*, Phil. Mag., **32**, 529 (1916).
- ¹⁹ C.J. Chapman and M.R.E. Proctor, *Nonlinear Rayleigh- Benard convection between poorly conducting boundaries*, J. Fluid Mech. **101**, 759 (1980).
- ²⁰ V.L. Gertsberg and G.I. Sivashinsky, *Large cells in nonlinear Rayleigh- Benard convection*, Prog. Theor. Phys. **66**, 1219 (1981).
- ²¹ M. C. Depassier, *A note on the free boundary condition in Rayleigh- Benard convection between insulating boundaries*, Phys. Letts. A, **102**, 359 (1984).
- ²² E. Knobloch, *Pattern selection in binary-fluid convection at positive separation ratios*, Phys. Rev. A **40**, 1549 (1989).

APPENDIX: THE CASE OF ARBITRARY BIOT NUMBERS B_ℓ, B_u

When the Biot numbers at the free surfaces, B_ℓ and B_u , are not both small the critical threshold for the instability is given by [compare eq. (19)]

$$M_u = \frac{b_1 M_l + b_2}{b_3 M_l + b_4}$$

where

$$b_1 = -8csk^4 - 8B_u(c^2 + s^2)k^3 + 8cs(B_u + 4c^2s^2)k^2 + 16B_u c^2 s^2 (c^2 + s^2)k$$

$$b_2 = 256c^3 s^3 k^4 + 128(B_\ell + B_u)c^2 s^2 (c^2 + s^2)k^3 + 256B_\ell B_u c^3 s^3 k^2$$

$$b_3 = (c^2 + s^2)k^3 - cs(k^4 + 3k^2) + 4c^3 s^3$$

$$b_4 = -8csk^4 - 8B_\ell(c^2 + s^2)k^3 + 8cs(B_\ell + 4c^2s^2)k^2 + 16B_\ell c^2 s^2 (c^2 + s^2)k$$

Again solving for $M_u(k; \alpha)$ and expanding about $k = 0$ we find that there is a root that is finite at $k = 0$ only if $B_\ell + B_u + B_\ell B_u = 0$ or if $B_\ell = B_u = 0$. Therefore, there is no longwave instability for any combination of Biot numbers and a weakly nonlinear stability analysis of the type derived in this paper is not relevant (except for $B_\ell \Rightarrow 0$ and $B_u \Rightarrow 0$, as studied in the main body of the paper).

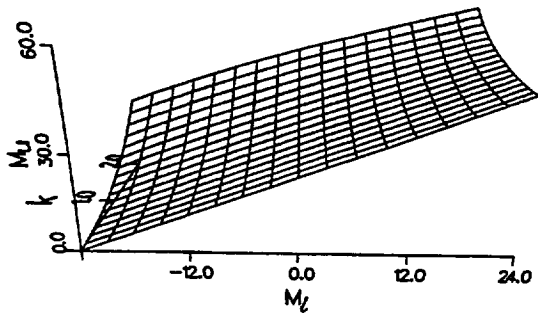


Figure 1.—The neutral surface $M_U = M_U(M_I, k)$ as given by eq. (19). In the case of longwave perturbations, $k = 0$, the cross-section of the surface is the straight line given by $M_U - M_I = 24$, eq. (25). The instability domain is above the surface.

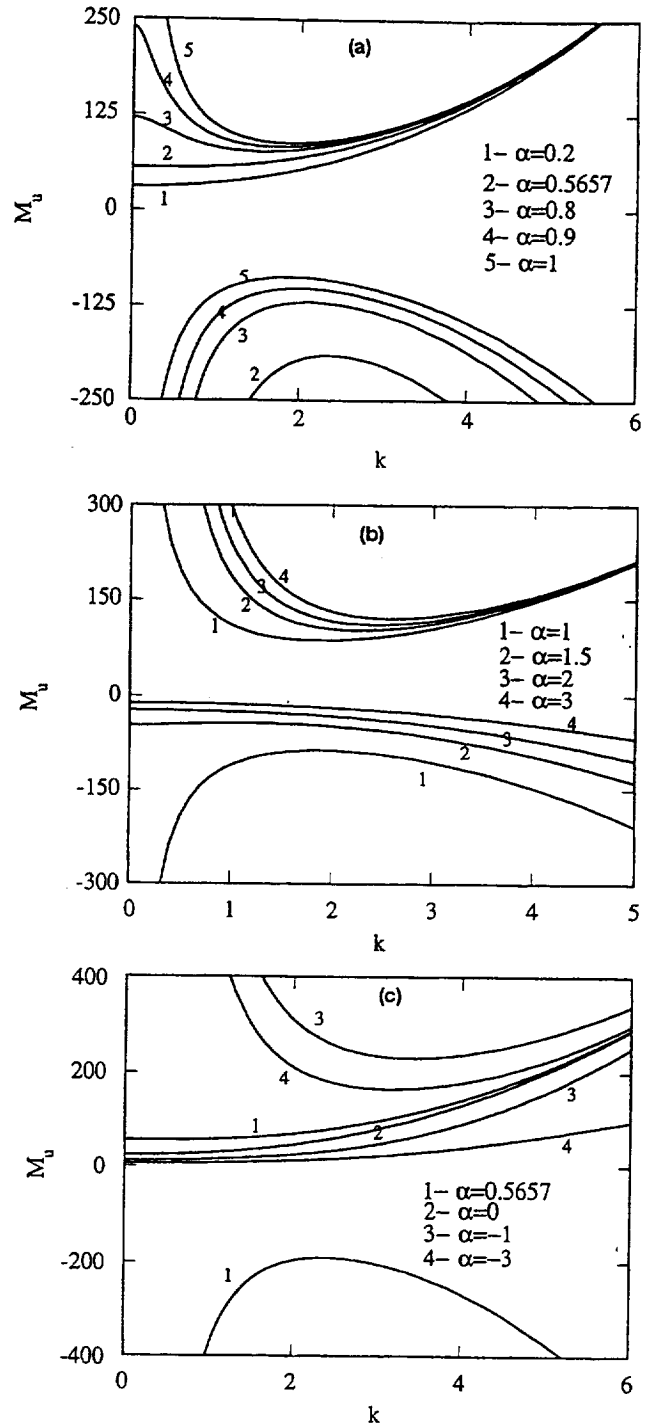


Figure 2.—The neutral stability curves for various values of the parameter α , as given by eq. (22). Two curve branches correspond to each value of $\alpha \neq 0$. (a) $0 < \alpha < 1$. If $M_U < 0$ the first instability is to finite wavenumber perturbations. For $M_U > 0$ the first instability is to zero wavenumber perturbations when $\alpha < 0.56574$ and to finite wavenumber otherwise. (b) $\alpha > 1$. For $M_U > 0$ the first instability is to finite wavenumber perturbations. For $M_U < 0$ the first instability is to zero wavenumber perturbations for $\alpha > 1.76759$ and to finite wavenumber otherwise. (c) $\alpha \leq 0$. The first instability is the longwave one. Note that the unstable domain lies between the two curves corresponding to the given value of α . There is only one curve corresponding to $\alpha = 0$.

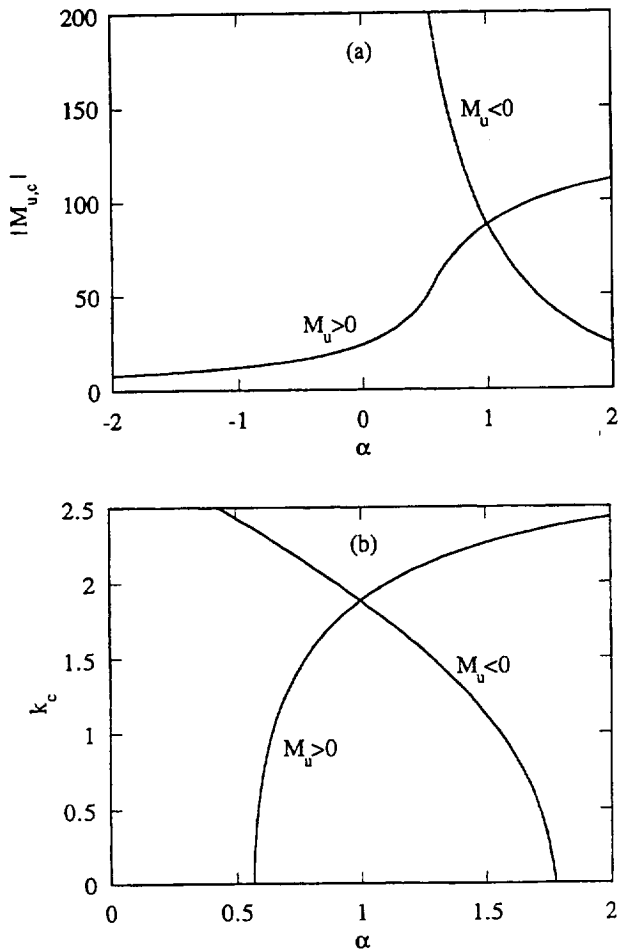


Figure 3.—(a) The critical value of the upper Marangoni number, $M_{u,c}$, as a function of the parameter α . Note that in the case of the negative Marangoni numbers the corresponding curve with the opposite sign is displayed. (b) The critical wavenumber of the perturbation, k_c , at which the first instability occurs. Note that in the case of $M_u > 0$, $k_c = 0$ for $\alpha < 0.56574$, while $k_c = 0$ for $\alpha > 1.76759$ when $M_u < 0$.

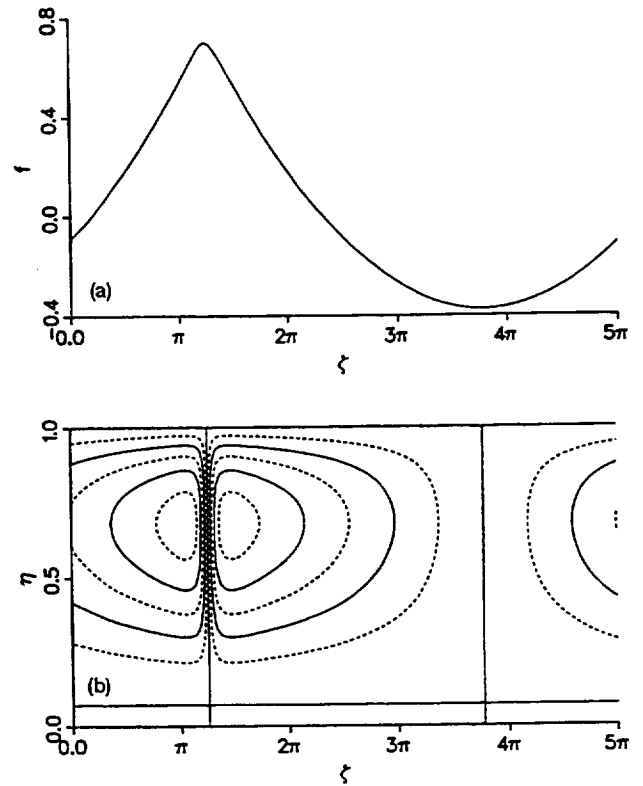


Figure 4.—The steady-state solution: (a) the temperature deviation from the equilibrium state; (b) the streamlines of the fluid flow, for eq. (57) with periodic boundary conditions, the initial condition $f_0(\zeta) = 0.01 \sin(2\pi\zeta/L)$, and $P = 5$, $\beta = 0$, $M_{u1} - M_{l1} = 6$, $L = 5\pi$, $M_{u0} = 54$, $M_{l0} = 30$. The direction of the flow in the cells at the free surfaces is from the hottest spot to the coldest one. The streamlines in the lower cell are not displayed due to its thinness. The two convective cells are counter-rotating.

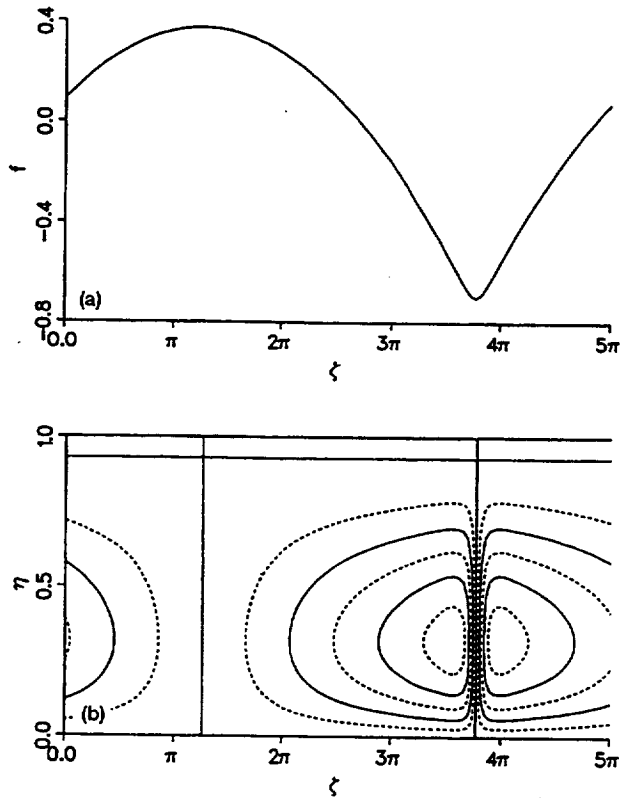


Figure 5.—The steady-state solution: (a) the temperature deviation from the equilibrium state and (b) the streamlines of the fluid flow, for eq. (57) with periodic boundary conditions, the initial condition $f_0(\zeta) = 0.01 \sin(2\pi\zeta/L)$, and $P = 5$, $\beta = 0$, $M_{U1} - M_{I1} = 6$, $L = 5\pi$, $M_{U0} = -30$, $M_{I0} = -54$. The direction of the flow in the cells at the free surfaces is from the coldest spot to the hottest one. The streamlines in the upper cell are not displayed due to its thinness. The two convective cells are counterrotating.

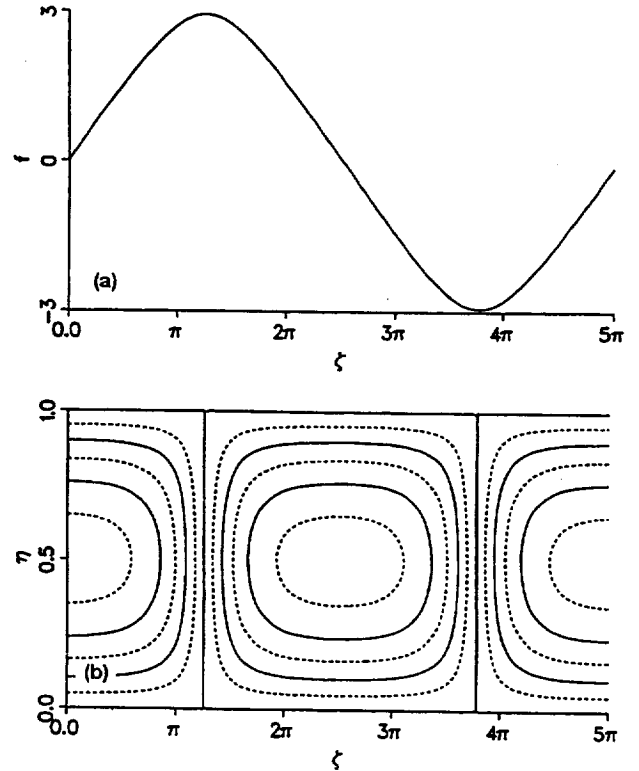


Figure 6.—The steady-state solution: (a) the temperature deviation from the equilibrium state; (b) the streamlines of the fluid flow, for eq. (57) with periodic boundary conditions, the initial condition $f_0(\zeta) = 0.01 \sin(2\pi\zeta/L)$, and $P = 5$, $\beta = 0$, $M_{U1} - M_{I1} = 6$, $L = 5$, $M_{U0} = 12$, $M_{I0} = -12$. The direction of the flow in the cells at the upper free surface is from the hottest spot to the coldest one, and at the lower free surface from the coldest spot to the hottest one. The streamlines of the flow are symmetric with respect to the midplane of the layer.

REPORT DOCUMENTATION PAGE

Form Approved
OMB No. 0704-0188

Public reporting burden for this collection of information is estimated to average 1 hour per response, including the time for reviewing instructions, searching existing data sources, gathering and maintaining the data needed, and completing and reviewing the collection of information. Send comments regarding this burden estimate or any other aspect of this collection of information, including suggestions for reducing this burden, to Washington Headquarters Services, Directorate for Information Operations and Reports, 1215 Jefferson Davis Highway, Suite 1204, Arlington, VA 22202-4302, and to the Office of Management and Budget, Paperwork Reduction Project (0704-0188), Washington, DC 20503.

1. AGENCY USE ONLY (Leave blank)		2. REPORT DATE July 1993	3. REPORT TYPE AND DATES COVERED Technical Memorandum	
4. TITLE AND SUBTITLE Marangoni Instability in a Liquid Layer With Two Free Surfaces			5. FUNDING NUMBERS WU-505-90-5K	
6. AUTHOR(S) Robert J. Deissler, Alexander Oron, and J.C. Duh				
7. PERFORMING ORGANIZATION NAME(S) AND ADDRESS(ES) National Aeronautics and Space Administration Lewis Research Center Cleveland, Ohio 44135-3191			8. PERFORMING ORGANIZATION REPORT NUMBER E-7862	
9. SPONSORING/MONITORING AGENCY NAME(S) AND ADDRESS(ES) National Aeronautics and Space Administration Washington, D.C. 20546-0001			10. SPONSORING/MONITORING AGENCY REPORT NUMBER NASA TM-106166 ICOMP-93-15	
11. SUPPLEMENTARY NOTES Robert J. Deissler, Institute for Computational Mechanics in Propulsion, NASA Lewis Research Center, (work funded under NASA Cooperative Agreement NCC3-233; Alexander Oron, Faculty of Mechanical Engineering, Technion-Israel Institute of Technology, Haifa, 32000, Israel; and J.C. Duh, Sverdrup Technology, Inc., Lewis Research Center Group, 2001 Aerospace Parkway, Brook Park, Oh 44142. ICOMP Program Director, Louis A. Povinelli, (216) 433-5818.				
12a. DISTRIBUTION/AVAILABILITY STATEMENT Unclassified - Unlimited Subject Category 34			12b. DISTRIBUTION CODE	
13. ABSTRACT (Maximum 200 words) We study the onset of the Marangoni instability in a liquid layer with two free nearly insulating surfaces heated from below. Linear stability analysis yields a condition for the emergence of a longwave or a finite wavelength instability from the quiescent equilibrium state. Using the method of asymptotic expansions we derive a weakly nonlinear evolution equation describing the spatiotemporal behavior of the velocity and temperature fields at the onset of the longwave instability. The latter is given by $\Delta M = 24$, ΔM being the difference between the upper and the lower Marangoni numbers. It is shown that in some parametric range one convective cell forms across the layer, while in other parametric domains two convective cells emerge between the two free surfaces.				
14. SUBJECT TERMS Thermocapillary convection; Marangoni instability; Liquid sheet; Weekly nonlinear analysis			15. NUMBER OF PAGES 26	
			16. PRICE CODE A03	
17. SECURITY CLASSIFICATION OF REPORT Unclassified	18. SECURITY CLASSIFICATION OF THIS PAGE Unclassified	19. SECURITY CLASSIFICATION OF ABSTRACT Unclassified	20. LIMITATION OF ABSTRACT	